Cortically coordinated NREM thalamocortical oscillations play an essential, instructive role in visual system plasticity

Jaclyn Durkin[a,1], Aneesha K. Suresh[b,1], Julie Colbath[c], Christopher Broussard[d], Jiaxing Wu[e], Michal Zochowski[f,g], and Sara J. Aton[c,2]

[a]Neuroscience Graduate Program, University of Michigan, Ann Arbor, MI 48109; [b]Committee on Computational Neuroscience, University of Chicago, Chicago, IL 60637; [c]Department of Molecular, Cellular, and Developmental Biology, University of Michigan, Ann Arbor, MI 48109; [d]Information Technology Advocacy and Research Support, College of Literature, Science, and the Arts, University of Michigan, Ann Arbor, MI 48109; [e]Program in Applied Physics, University of Michigan, Ann Arbor, MI 48109; [f]Program in Biophysics, University of Michigan, Ann Arbor, MI 48109; and [g]Department of Physics, University of Michigan, Ann Arbor, MI 48109

Two long-standing questions in neuroscience are how sleep promotes brain plasticity and why some forms of plasticity occur preferentially during sleep vs. wake. Establishing causal relationships between specific features of sleep (e.g., network oscillations) and sleep-dependent plasticity has been difficult. Here we demonstrate that presentation of a novel visual stimulus (a single oriented grating) causes immediate, instructive changes in the firing of mouse lateral geniculate nucleus (LGN) neurons, leading to increased firing-rate responses to the presented stimulus orientation (relative to other orientations). However, stimulus presentation alone does not affect primary visual cortex (V1) neurons, which show response changes only after a period of subsequent sleep. During poststimulus nonrapid eye movement (NREM) sleep, LGN neuron overall spike-field coherence (SFC) with V1 delta (0.5–4 Hz) and spindle (7–15 Hz) oscillations increased, with neurons most responsive to the presented stimulus showing greater SFC. To test whether coherent communication between LGN and V1 was essential for cortical plasticity, we first tested the role of layer 6 corticothalamic (CT) V1 neurons in coherent firing within the LGN-V1 network. We found that rhythmic optogenetic activation of CT V1 neurons dramatically induced coherent firing in LGN neurons and, to a lesser extent, in V1 neurons in the other cortical layers. Optogenetic interference with CT feedback to LGN during poststimulus NREM sleep (but not REM or wake) disrupts coherence between LGN and V1 and also blocks sleep-dependent response changes in V1. We conclude that NREM oscillations relay information regarding prior sensory experience between the thalamus and cortex to promote cortical plasticity.

sleep | vision | thalamocortical | plasticity | coherence

Converging behavioral (1), biochemical (2–4), neuroanatomical (5), and electrophysiological (2, 6–8) evidence supports the idea that following novel sensory experiences, sleep can promote cortical plasticity. The sleep-dependent mechanisms driving these changes have remained elusive. Sleep-associated changes in network activity (1, 6, 7, 9, 10), neuromodulator tone (11), transcription (4), translation (4), and protein phosphorylation (2, 3) have all been correlated with cortical plasticity following novel experiences (12). In recent years, neuroscientists have speculated that the high-amplitude, low-frequency thalamocortical oscillations that characterize nonrapid eye movement (NREM) sleep play a critical role in promoting sensory cortical plasticity and learning (12). While it has been hypothesized that such NREM oscillations promote general synaptic "downscaling" (13), converging data suggest that they could instead promote synaptic strengthening (5–7, 9). While rhythmic stimulation of the cortex at frequencies meant to mimic NREM oscillations (1–2 Hz) is sufficient to promote cortical plasticity and learning (9, 10), it is unclear whether naturally occurring

oscillations are necessary for sleep-dependent processes. Another critical question is whether NREM oscillations play an instructive role in experience-initiated plasticity—i.e., whether these oscillations relay information about prior experience through thalamocortical circuitry.

Orientation-specific response potentiation (OSRP) in mouse primary visual cortex (V1) (14) is initiated by a novel visual stimulus (a flickering grating of a single orientation) presented over a period of several minutes (7). OSRP is expressed in V1 several hours later, as enhanced neuronal responses to stimuli of the same orientation; critically, sleep deprivation following visual experience prevents OSRP consolidation (7, 8). Recent data suggest that OSRP is mediated by potentiation of lateral geniculate nucleus (LGN) synapses in V1 (15). To clarify the role of thalamocortical and corticothalamic (CT) communication in OSRP consolidation, we first tested how visual experience alone affected neuronal firing and OSRP in both LGN and V1 neurons and then determined how coherent firing between the two areas was affected during subsequent sleep. We also tested the effects of optogenetic manipulations of layer 6 corticothalamic (CT) neurons, aimed at either mimicking or disrupting NREM sleep oscillations, on both neuronal firing patterns and OSRP following visual experience.

Significance

Previous studies have demonstrated a role of state-specific neural activity in plasticity; however, a mechanism for these changes has yet to be elucidated. Here, we demonstrate that sensory response changes occur in thalamic neurons immediately following novel visual experience, but that subsequent nonrapid eye movement (NREM) oscillations are required for subsequent response changes in the primary visual cortex (V1). Consequently, we show that disruption of NREM oscillations specifically blocks sleep-dependent plasticity in V1. We conclude that following a novel sensory experience, neural activity patterns unique to NREM facilitate transfer of information from the visual thalamus to the V1, leading to adaptive response changes in V1 neurons.

Results

LGN, but Not V1, Neurons Show Immediate Orientation-Specific Response Changes Following Visual Stimulation. Previous studies [by our laboratory (7, 8) and others (14)] have demonstrated that orientation preference in V1 neurons is unchanged immediately after presentation of a single oriented grating stimulus, even for stimulus durations of up to an hour. To test whether LGN neurons are similarly unaffected across stimulus presentation, we generated orientation tuning curves for individual V1 and LGN neurons in anesthetized mice before and after a 30-min grating presentation. Surprisingly, many LGN neurons showed dramatic orientation-specific response changes during this treatment (e.g., the ratio of neuronal firing rate for X° over the neuronal firing rate for the orthogonal, X + 90°). These increases in X°/X + 90° were present across a number of recordings for different presented stimulus orientations (Fig. 1 and *SI Appendix*, Figs. S1 and S2; n = 147 neurons from seven experiments), but, consistent with our previous findings (7), were not seen in V1 neurons recorded from the same mice (n = 32 neurons). Among many of the recorded LGN neurons, visually evoked firing-rate responses increased significantly across the 30-min grating presentation, a phenomenon that we had not previously seen in V1 (8) (Fig. 2A). The amount that individual neuron firing rates changed across stimulus presentation, while heterogeneous, predicted the amount of change in X°/X + 90° after stimulus presentation (Fig. 2B and *SI Appendix*, Fig. S6A). This rapid response change did not result in an increase in the proportion of LGN neurons selective for the presented stimulus orientation (*SI Appendix*, Figs. S1 and S2); rather, neuronal firing-rate responses to X° selectively increased (e.g., relative to X + 90° and X ± 45°).

To better understand the relationship of these firing-rate changes to OSRP seen in V1 across a period of poststimulus sleep, we simultaneously recorded both LGN and V1 neurons in nonanesthetized animals during and after presentation of a grating at the beginning of the rest phase (CT0). Here again, we found that firing-rate responses increased significantly across stimulus presentation in LGN, but not in V1 (Fig. 2C). Firing increases were not seen in LGN neurons recorded from mice presented with a blank screen [not significant (N.S.); Fig. 2C]. Firing-rate increases among LGN neurons during stimulus presentation predicted increases in X°/X + 90° measured across the rest period (Fig. 2D and *SI Appendix*, Fig. S6B). Critically, as we had previously shown for V1 neurons following OSRP induction (8), firing rates in LGN neurons remained elevated during poststimulus NREM sleep (Fig. 2E). Taken together, these data suggest that

oriented grating presentation leads to (*i*) rapid changes in X°/X + 90° in LGN neurons and (*ii*) long-lasting changes in firing of LGN neurons during subsequent NREM sleep.

LGN Neurons Show Increased Spike-Field Coherence with NREM Thalamocortical Oscillations During OSRP Consolidation. OSRP is expressed in V1 only after several hours of poststimulus sleep; critically, sleep deprivation following visual experience prevents OSRP consolidation (7, 8) (*SI Appendix*, Fig. S3). To assess whether communication between LGN and V1 changes during poststimulus sleep, we continuously recorded LGN and V1 neuronal firing and corresponding local field potential (LFP) activity (*SI Appendix*, Figs. S4 and S5). Recordings spanned a 24-h period of baseline sleep and wake, a 30-min stimulus presentation, and a subsequent 12-h OSRP consolidation window. We then characterized the temporal relationships [in the form of spike-field coherence (SFC)] between LGN neuronal firing and V1 LFP oscillations during OSRP consolidation (Fig. 3). LGN neuron SFC with V1 delta and spindle oscillations increased during NREM in the hours following oriented grating presentation (Fig. 3B and *SI Appendix*, Fig. S6C).

We also tested whether LGN neurons underwent an increase in coherent firing during NREM per se by assessing the periodicity of firing before and after oriented grating exposure. We found that following stimulus presentation, coherent LGN neuronal firing in the delta frequency band predicted the extent of their OSRP across the poststimulus period (Fig. 3C and *SI Appendix*, Fig. S6D). These data suggest that, as is true for V1 neurons (7), waking visual experience leads to changes in LGN neuron coherent firing during subsequent NREM sleep. Because OSRP is present only in the LGN immediately following experience, we hypothesized that LGN-V1 coherence during NREM oscillations could promote sleep-dependent OSRP consolidation in V1.

Layer 6 CT Input Is Sufficient to Drive Coherent Firing in the LGN-V1 Network. CT input is necessary for coordinating NREM delta and spindle oscillations within thalamic circuits (16, 17). Thus, CT-mediated coordination might be critical for promoting the observed changes in LGN-V1 coherence during poststimulus NREM sleep. To test the sufficiency of V1 layer 6 (L6) CT input to drive coherent firing in LGN and V1, we recorded LGN and V1 firing patterns in transgenic mice expressing channelrhodopsin 2 (ChR2) in L6 CT neurons (*Ntsr1:ChR2*) (Fig. 4 *A*, *B*, *G*, and *H* and *SI Appendix*, Fig. S7). After recording baseline activity in both areas, we measured changes in firing rhythmicity in response to rhythmic optogenetic activation of V1 L6 CT neurons across a range
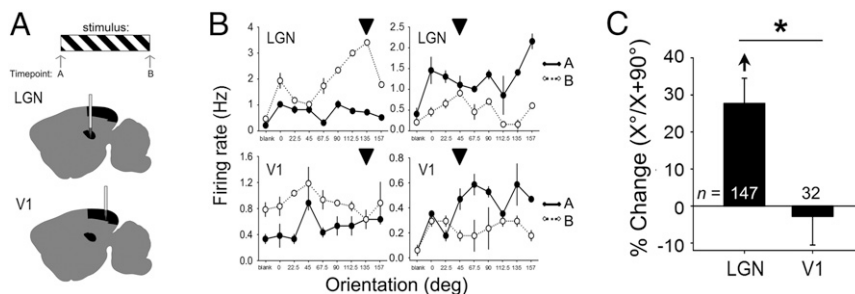
Fig. 1. Visual experience immediately alters response properties in LGN, but not in V1, neurons. (*A*) Visual responses of LGN and V1 neurons were recorded from mice under isoflurane anesthesia. At time point A, mice were presented randomly with a series of oriented full-field grating stimuli (0, 22.5, 45, 67.5, 90, 112.5, 135, and 157.5 degrees) and a blank screen (bl) to assess baseline orientation tuning and visual responsiveness. One stimulus was chosen at random and presented for a 30-min period. At time point B, visual response properties were reassessed. (*B*) Tuning curves for representative LGN neurons (*Top*) show increased relative responses to the presented orientation (vs. other orientations; presented stimulus indicated with arrowhead) from time point A (solid line) to time point B (dotted line). Consistent with our prior findings (7), V1 neurons (*Bottom*) do not show an enhanced response to the presented orientation immediately following stimulus presentation. Values indicate mean firing-rate response (±SEM) to each stimulus. (*C*) Immediately following visual stimulus presentation, LGN neurons (but not V1 neurons) showed a significant increase in relative responsiveness to the presented stimulus orientation [relative to the orthogonal orientation (X°/X + 90°); arrow indicates P < 0.05, repeated measures (RM) ANOVA on ranks; *P < 0.05 for LGN vs. V1 neurons].
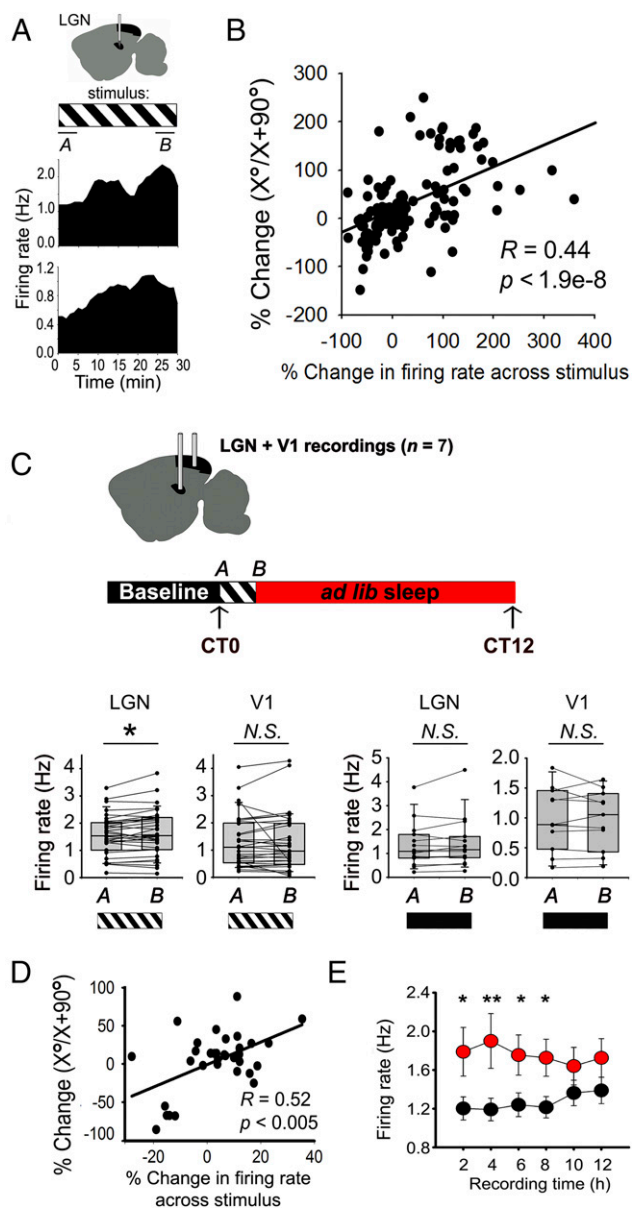
Fig. 2. Stimulus-induced firing enhancement in LGN neurons predicts response changes and persists during subsequent NREM sleep. (A) Two representative LGN neurons recorded from an anesthetized mouse show firing-rate increases across the 30-min stimulus presentation (mean rate plotted in 1-min bins). (B) Firing-rate increases predicted the change in X°/X + 90° (i.e., OSRP) across stimulus presentation. Pearson product moment R and P values are shown for 147 LGN neurons. (C, Top) Mice implanted with electrodes targeting both LGN and V1 were recorded over a 24-h baseline period, presented with an oriented grating at CT0, and then allowed 12 h of ad libitum sleep. Visual response properties were assessed at CT0 and CT12. (C, Bottom Left) V1 neurons showed no change in firing rate between the first and last 5 min of the 30-min grating presentation (time point A and time point B, respectively, N.S., Wilcoxon signed rank test, n = 34 neurons from six mice). However, LGN neuronal firing rates increased significantly (P = 0.018, Wilcoxon signed rank test, n = 35 neurons). (C, Bottom Right) Neither V1 nor LGN neurons showed a significant change in firing rate between the first and last 5 min of a 30-min blank screen presentation (N.S., Wilcoxon signed rank test, n = 16 and 11 neurons, respectively, from three experiments). (D) As was true in anesthetized recordings, firing-rate increases in LGN neurons across stimulus presentation predicted OSRP across the day. Pearson product moment R and P values are shown for 35 stably recorded LGN neurons. (E) Compared with baseline recording (black), LGN neuron firing rates during the first 8 h of poststimulus NREM (red) remained significantly elevated (two-way RM ANOVA, treatment × time interaction P < 0.001; *P < 0.05, **P < 0.01). N.S., not significant.

of frequencies: 0.5, 1, 2, 3, and 4 Hz. In both V1 and LGN recordings, we observed phase-locking of both neurons' firing and LFP activity to optogenetically induced rhythms of CT activity (Fig. 4 B and H). Only a subset of stimulation frequencies (1, 2, and 3 Hz) increased V1 neuron firing coherence significantly from baseline (Fig. 4C). In contrast, stimulation at all frequencies increased LGN neuron firing coherence and led to more pronounced (i.e., higher amplitude) firing rhythms compared with those induced in V1 (Fig. 4I). The proportion of LGN neurons significantly affected by optogenetic stimulation of V1 CT neurons (Fig. 4L) was also much greater than the proportion of neurons affected in V1 (Fig. 4F).

Optogenetic stimulation of L6 CT neurons similarly affected the rhythmicity of LFP activity in both V1 (Fig. 4 D and E) and LGN (Fig. 4 J and K). Optogenetic activation of V1 CT neurons also induced higher-frequency (11–15 Hz) spindle-like LFP events in V1 (*SI Appendix*, Fig. S8A). These events were time-locked to rhythmic optogenetic stimulation and varied in density and duration based on stimulation frequency (*SI Appendix*, Fig. S8 B and C).

Optogenetic Inhibition of L6 CT Neurons Disrupts V1-LGN Coherence During NREM Sleep. We next tested whether optogenetic inhibition of L6 CT neurons could disrupt coherent NREM oscillations following induction of OSRP. To do this, we virally transduced L6 CT neurons in V1 with archaerhodopsin3 (Arch) (18) in L6 CT neurons in V1 (*SI Appendix*, Fig. S9). Light delivery to V1 of transduced mice reliably and reversibly suppressed firing in the majority of V1 L6 neurons (and target neurons in the LGN) over a timescale of seconds to minutes (Fig. 5A and *SI Appendix*, Fig. S10). NREM-targeted light delivery in the hours following visual stimulus presentation significantly reduced delta and spindle-frequency LFP power in V1, relative to baseline NREM sleep (Fig. 5B and *SI Appendix*, Fig. S11). Spindle-frequency coherence between LGN LFPs and V1 LFPs was significantly reduced during NREM-targeted inhibition of V1 CT neurons (Fig. 5C). This was associated with a disruption in the temporal relationship between V1 and LGN fields, leading to longer delays (relative to lag times seen at baseline) between V1 and LGN spindle-frequency activity (an effect not seen in
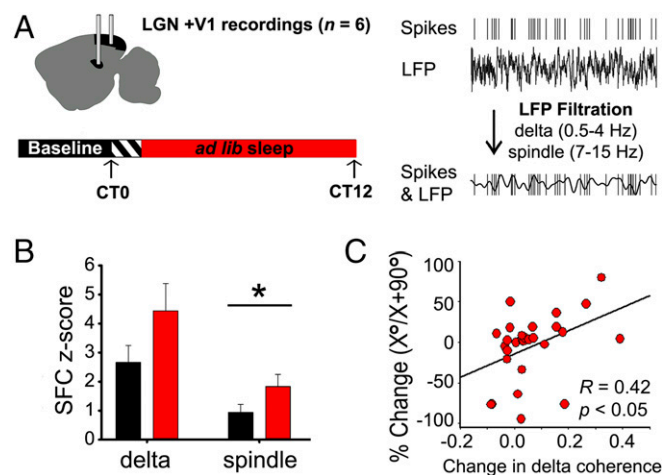
Fig. 3. LGN neurons show increased SFC with V1 NREM oscillations following stimulus presentation. (A) Mice implanted with electrodes targeted to LGN and V1 were recorded as described in Fig. 2C. LGN SFC with V1 oscillations was calculated during NREM at baseline and after stimulus presentation. (B) Following stimulus presentation, LGN neurons showed significantly increased SFC with V1 LFPs filtered at spindle frequency (*P = 0.01, Wilcoxon signed rank test). There was a similar trend for increased SFC in the delta frequency band (P = 0.088, Wilcoxon signed rank test). (C) Increases in LGN firing periodicity at delta frequencies during NREM predicted their ORSP across the day. Pearson product moment R and P values are shown for 35 stably recorded LGN neurons.
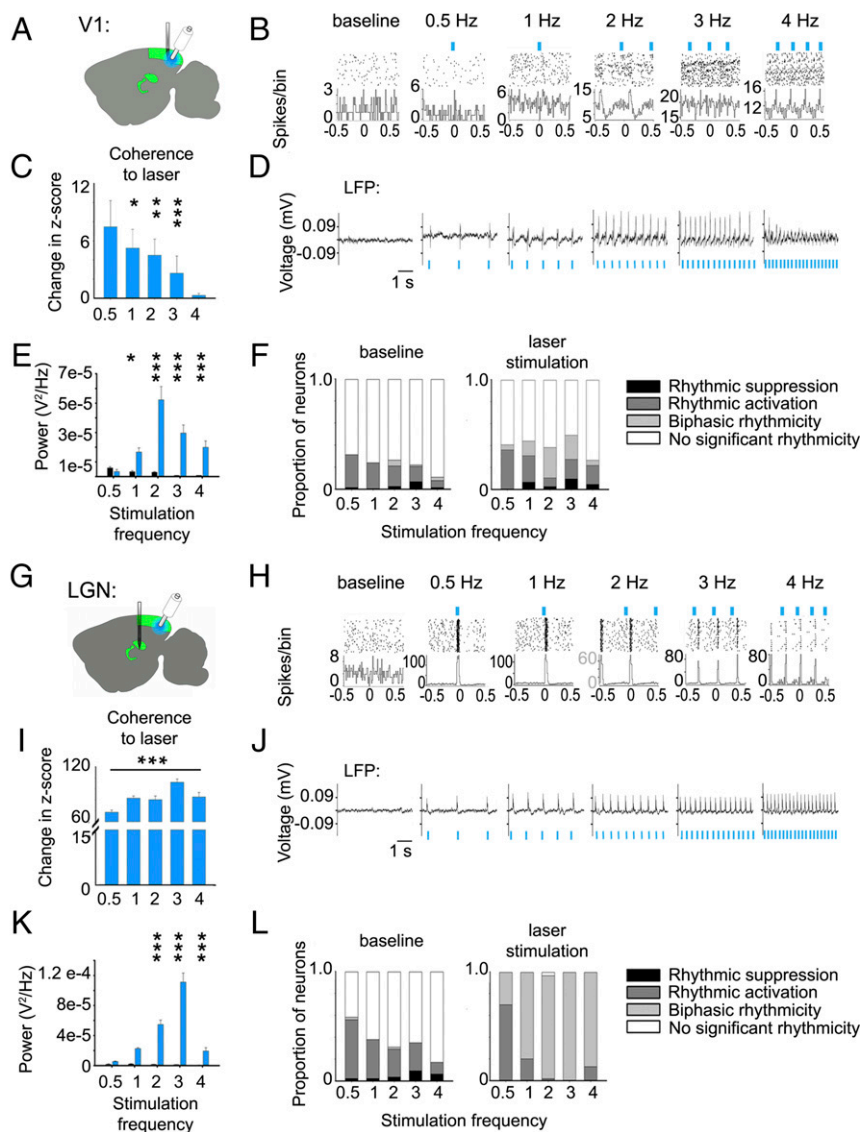
Fig. 4. Stimulation of ChR2-expressing CT neurons induced coherent firing in V1 and LGN. (*A*) For V1 recordings from anesthetized *Ntsr1::ChR2* mice, a 32-channel silicone probe was lowered into the V1 until stable recordings were obtained, and an optical fiber was targeted to V1 L6. Neuronal responses were aggregated across all layers of the visual cortex. (*B*) Peri-event spike rasters and histograms are shown for a representative neuron at baseline and during optogenetic stimulation of V1 L6. (*C*) V1 neurons showed increased coherent firing at the frequency of optogenetic stimulation compared with baseline. *$P <$ 0.05, **$P <$ 0.01, and ***$P <$ 0.001, Wilcoxon signed rank test. (*D*) LFP activity is shown at baseline and during optogenetic stimulation. (*E*) LFP power at the frequency of stimulation (blue bars) was significantly increased from baseline (black bars) values during stimulation. *$P <$ 0.05 and ***$P <$ 0.001, Holm–Sidak post hoc test vs. baseline. (*F*) The proportion of V1 neurons that showed statistically significant ($P <$ 0.01) periodic suppression and activation are shown for each frequency during baseline (*Left*) and during optogenetic stimulation (*Right*). (*G*) For LGN neuronal recordings in anesthetized *Ntsr1::ChR2* mice, a 32-channel silicone probe was lowered into LGN until stable recordings were obtained, and an optical fiber was targeted to V1 L6. (*H–L*) Data for LGN spiking and LFP activity are shown as in *B–F*. For *L*, all LGN neurons showed significant rhythmicity during optogenetic stimulation of L6 CT neurons.

the absence of CT inhibition; Fig. 5*D*; N.S. for delta frequency activity, *SI Appendix*, Fig. S12). LGN neuron SFC with V1 delta and spindle oscillations was also significantly reduced during V1 CT inhibition (Fig. 5*E*). Taken together, these changes demonstrate that inhibition of L6 CT neurons desynchronizes NREM oscillations and thalamocortical communication during OSRP consolidation.

Optogenetic Inhibition of CT Neurons During NREM, but Not REM or Wake, Disrupts V1 Plasticity. We next tested the necessity of state-specific CT activity for consolidation of OSRP in V1. Following presentation of a visual stimulus to induce OSRP, Arch-expressing mice underwent a 6-h period of state-targeted V1 CT neuron inhibition during bouts of NREM, REM, or wake (Fig. 6*A* and *SI Appendix*, Fig. S15). This intervention had no

significant effect on sleep architecture across either the 6-h period of optogenetic inhibition or the 6 h of subsequent recovery sleep (N.S., two-way ANOVA; *SI Appendix*, Figs. S16 and S17). There were no significant differences in V1 OSRP between control mice without CT neuron inhibition, mice with REM- or wake-targeted inhibition of CT neurons, and mice expressing a control (YFP) transgene following NREM-targeted light delivery to V1 (N.S., Holm–Sidak test). However, inhibition of CT neurons during NREM blocked OSRP in a manner similar to sleep deprivation ($P <$ 0.001, ANOVA; Fig. 6*B* and *SI Appendix*, Figs. S19 and S20). Similarly, the distribution of orientation preference changed across a period of sleep (leading to a greater proportion of neurons preferring X°) in control mice without CT neuron inhibition, mice with REM- or wake-targeted inhibition of CT
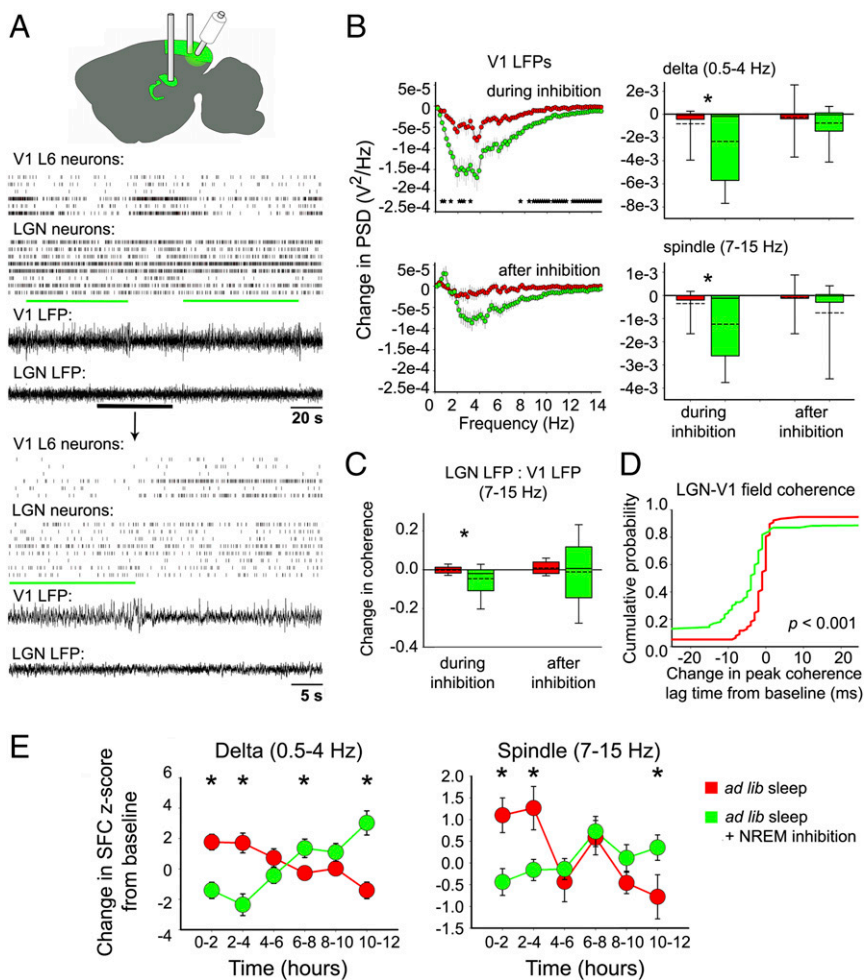
Fig. 5. NREM-targeted optogenetic inhibition of V1 L6 CT neurons disrupts coherent thalamocortical oscillations. (*A*) LGN and V1 activity was simultaneously recorded in *Ntsr1-cre* transgenic mice transduced with Arch-GFP. L6 V1 CT neurons were optogenetically inhibited across bouts of NREM sleep in the first 6 h of the poststimulus ad libitum sleep period. Light delivery reliably inhibited L6 neuronal firing and slightly reduced firing in LGN neurons. (*B, Left*) V1 power spectral density during NREM-targeted L6 inhibition (expressed as a change from baseline; *n* = 64 LFPs from 11 mice, green) was significantly reduced relative to that of no-laser (noninhibited) control mice (*n* = 76 LFPs from 14 mice, red; *P < 0.05 for no-laser vs. inhibited conditions, Bonferroni-corrected Student's *t* test for each frequency value). (*B, Right*) Total integrated spectral power changes (from baseline) across delta (0.5–4 Hz) and spindle (7–15 Hz) frequency bands significantly decreased during inhibition (green; * indicates *P* < 0.01 and *P* < 0.001, respectively) compared with no-laser control mice (red). Power recovered to normal levels after the 6-h inhibition period (N.S., Mann–Whitney rank sum test). (*C*) Spindle-frequency coherence decreased between V1 and LGN LFPs during NREM inhibition [*n* = 77 LFP pairs recorded across both inhibition and control conditions in four mice; *P* < 0.001 (indicated by *) and *P* = 0.786, respectively, for during and after 6-h NREM-targeted inhibition; Mann–Whitney rank sum test]. (*D*) NREM-targeted inhibition caused an increase in the time lag between V1 and LGN LFPs at their maximum spindle-frequency coherence, relative to baseline (*P* < 0.001, Kolmogorov–Smirnov test for inhibition vs. no-laser conditions). (*E*) NREM-targeted inhibition of L6 CT neurons decreased interareal SFC between LGN and V1. LGN spike to V1 LFP SFC at delta frequency: condition × time interaction *P* < 0.001; at spindle frequency: main effect of time *P* = 0.01 and condition × time interaction *P* < 0.001; two-way RM ANOVA; *n* = 54 neurons from seven mice and 40 neurons from five mice for no-laser control and inhibition conditions, respectively. V1 spike and LGN LFP SFC at delta frequency: main effect of time *P* < 0.05 and condition × time interaction *P* < 0.001 and at spindle frequency: N.S.; *n* = 29 neurons from six mice and 17 neurons from four mice for no-laser control and inhibition conditions, respectively. *P < 0.05, Holm–Sidak post hoc test.

neurons, and mice expressing a control (YFP) transgene, but not mice with NREM-targeted inhibition (*SI Appendix*, Fig. S20). NREM-targeted CT inhibition appeared to specifically disrupt sleep-associated OSRP consolidation, as there were no immediate effects of L6 CT neuron inhibition on orientation tuning in any layer of V1 (*SI Appendix*, Fig. S14). Thus, these data suggest that CT coordination of NREM oscillations in the LGN-V1 network plays a critical role in promoting sleep-dependent V1 OSRP.

Discussion

Our present data show that novel visual experience rapidly alters response properties in LGN neurons to enhance their responsiveness in favor of the presented stimulus orientation. This change is selective, occurring before expression of V1 OSRP, which relies on

subsequent sleep (7) (*SI Appendix*, Fig. S3). This experience also alters the temporal relationship between LGN neuron firing and V1 activity during subsequent NREM oscillations.

Previous studies have found that a subset of mouse LGN neurons shows orientation-selective responses (19–21). However, until now, it was unknown whether orientation-selective responses in the LGN (like that in the V1) can change in response to visual experience. Our data suggest that sensory response plasticity does occur in LGN neurons. Prior work in the somatosensory system (22, 23) suggested that thalamic neurons can change their response properties rapidly following disruption of peripheral sensory input. These data demonstrate that, following novel sensory experience, thalamic neurons in the visual pathway also show rapid response plasticity and that these changes precede response plasticity in V1.

NEUROSCIENCE
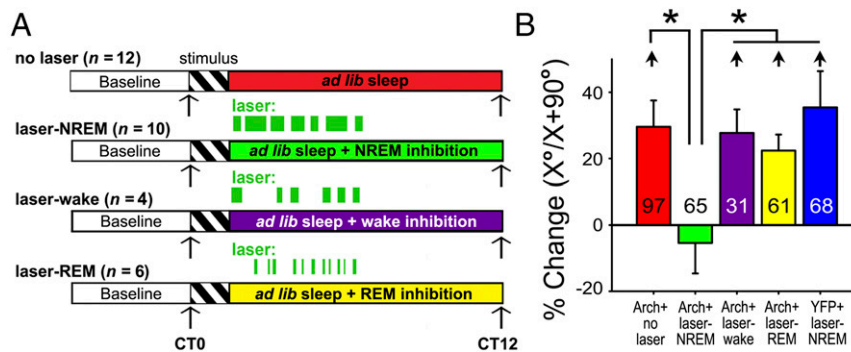
Fig. 6. NREM-targeted inhibition of CT neurons disrupts consolidation of V1 response plasticity after visual experience. (*A*) Experimental paradigm for evaluating the effects of poststimulus-state–targeted optogenetic inhibition of V1 CT neurons on OSRP consolidation. (*B*) NREM-targeted inhibition of V1 CT neurons (laser-NREM) reduced OSRP in V1, while inhibition in other states did not affect OSRP. *$P < 0.001$, Dunn's post hoc test versus no-laser controls, laser-wake, laser-REM, and YFP-expressing control mice with light delivery targeted to V1 during NREM ($P < 0.001$; Kruskal–Wallis ANOVA on ranks). With the exception of neurons recorded from mice with NREM-targeted inhibition, neurons recorded from all groups showed a significant increase in relative responsiveness to the presented stimulus orientation [relative to the orthogonal orientation (X°/X + 90°); short arrows indicate $P < 0.05$, RM ANOVA on ranks].

Why does subsequent OSRP in V1 require poststimulus sleep? One possibility is that information is relayed between LGN and V1 during poststimulus NREM, which in turn drives plasticity in the cortex. This interpretation is consistent with what is known about the circuit-level mechanisms of OSRP consolidation. LGN-to-V1 long-term potentiation (LTP) and OSRP are mutually occluding in vivo (15), suggesting that potentiation of thalamocortical synapses underlies OSRP consolidation in V1. We have previously shown that OSRP consolidation is dependent on poststimulus sleep (7, 8). Here we show that in freely sleeping mice, disruption of V1 CT neuron activity during NREM oscillations is sufficient to block OSRP consolidation. While CT neurons also influence the firing of neurons in the other layers of V1 (24), we find that their effects on firing among LGN neurons are much more widespread and dramatic (Fig. 4). We also find that optogenetic inhibition of CT neurons disrupts communication between LGN and V1 during NREM delta and spindle oscillations (Fig. 5). Because we have previously shown that coherent firing of V1 neurons during NREM oscillations predicts the extent of OSRP consolidation (7), a parsimonious interpretation is that thalamocortical coherence during NREM is essential for promoting OSRP in V1. Based on our current data, we conclude that information regarding stimulus characteristics of prior experience is relayed between the thalamus and cortex during subsequent NREM oscillations.

We find that V1-to-LGN CT communication, which coordinates thalamocortical oscillations associated with NREM sleep, plays an essential role for consolidating sensory response plasticity in V1.

Materials and Methods

All animal procedures were approved by the University of Michigan Institutional Animal Care and Use Committee. For anesthetized recording of visual response properties, or effects of L6 stimulation, 2- to 3-mo-old mice were anesthetized with isoflurane, and a 32-site silicon probe was inserted into either V1 or LGN for neuronal recording. For chronic recording from behaving mice, 2-mo-old mice were implanted with drivable headstages composed of two bundles with seven stereotrodes each, using previously described methods (7). Signals from each electrode were split and differentially filtered to obtain spike data and LFP data at each recording site. Individual neurons were tracked throughout the experiment as described previously (7, 25). Complete materials and methods are in *SI Appendix, SI Materials and Methods*.

1. Huber R, Ghilardi MF, Massimini M, Tononi G (2004) Local sleep and learning. *Nature* 430:78–81.
2. Aton SJ, et al. (2009) Mechanisms of sleep-dependent consolidation of cortical plasticity. *Neuron* 61:454–466.
3. Dumoulin MC, et al. (2015) Extracellular signal-regulated kinase (ERK) activity during sleep consolidates cortical plasticity in vivo. *Cereb Cortex* 25:507–515.
4. Seibt J, et al. (2012) Protein synthesis during sleep consolidates cortical plasticity in vivo. *Curr Biol* 22:676–682.
5. Yang G, et al. (2014) Sleep promotes branch-specific formation of dendritic spines after learning. *Science* 344:1173–1178.
6. Aton SJ, et al. (2013) Visual experience and subsequent sleep induce sequential plastic changes in putative inhibitory and excitatory cortical neurons. *Proc Natl Acad Sci USA* 110:3101–3106.
7. Aton SJ, Suresh A, Broussard C, Frank MG (2014) Sleep promotes cortical response potentiation following visual experience. *Sleep* 37:1163–1170.
8. Durkin J, Aton SJ (2016) Sleep-dependent potentiation in the visual system is at odds with the synaptic homeostasis hypothesis. *Sleep* 39:155–159.
9. Chauvette S, Seigneur J, Timofeev I (2012) Sleep oscillations in the thalamocortical system induce long-term neuronal plasticity. *Neuron* 75:1105–1113.
10. Miyamoto D, et al. (2016) Top-down cortical input during NREM sleep consolidates perceptual memory. *Science* 352:1315–1318.
11. Gais S, Born J (2004) Low acetylcholine during slow-wave sleep is critical for declarative memory consolidation. *Proc Natl Acad Sci USA* 101:2140–2144.
12. Aton SJ (2013) Set and setting: How behavioral state regulates sensory function and plasticity. *Neurobiol Learn Mem* 106:1–10.
13. Tononi G, Cirelli C (2003) Sleep and synaptic homeostasis: A hypothesis. *Brain Res Bull* 62:143–150.
14. Frenkel MY, et al. (2006) Instructive effect of visual experience in mouse visual cortex. *Neuron* 51:339–349.
15. Cooke SF, Bear MF (2010) Visual experience induces long-term potentiation in the primary visual cortex. *J Neurosci* 30:16304–16313.
16. Contreras D, Destexhe A, Sejnowski TJ, Steriade M (1996) Control of spatiotemporal coherence of a thalamic oscillation by corticothalamic feedback. *Science* 274:771–774.
17. Timofeev I, Steriade M (1996) Low-frequency rhythms in the thalamus of intact-cortex and decorticated cats. *J Neurophysiol* 76:4152–4168.
18. Chow BY, et al. (2010) High-performance genetically targetable optical neural silencing by light-driven proton pumps. *Nature* 463:98–102.
19. Piscopo DM, El-Danaf RN, Huberman AD, Niell CM (2013) Diverse visual features encoded in mouse lateral geniculate nucleus. *J Neurosci* 33:4642–4656.
20. Zhao X, Chen H, Liu X, Cang J (2013) Orientation-selective responses in the mouse lateral geniculate nucleus. *J Neurosci* 33:12751–12763.
21. Tang J, Ardila Jimenez SC, Chakraborty S, Schultz SR (2016) Visual receptive field properties of neurons in the mouse lateral geniculate nucleus. *PLoS One* 11:e0146017.
22. Nicolelis MA, Lin RC, Woodward DJ, Chapin JK (1993) Induction of immediate spatiotemporal changes in thalamic networks by peripheral block of ascending cutaneous information. *Nature* 361:533–536.
23. Krupa DJ, Ghazanfar AA, Nicolelis MA (1999) Immediate thalamic sensory plasticity depends on corticothalamic feedback. *Proc Natl Acad Sci USA* 96:8200–8205.
24. Bortone DS, Olsen SR, Scanziani M (2014) Translaminar inhibitory cells recruited by layer 6 corticothalamic neurons suppress visual cortex. *Neuron* 82:474–485.
25. Ognjanovski N, et al. (2017) Parvalbumin-expressing interneurons coordinate hippocampal network dynamics required for memory consolidation. *Nat Commun* 8:15039.